Solution conformations of a linked construct of the Zika virus NS2B-NS3 protease

Mithun C. Mahawaththa,[1] Benjamin J. G. Pearce,[1] Monika Szabo,[2] Bim Graham,[2] Christian D. Klein,[3] Christoph Nitsche,[1,*] Gottfried Otting[1,*]

[1] Research School of Chemistry, The Australian National University, Canberra, ACT 2601, Australia

[2] Monash Institute of Pharmaceutical Sciences, Monash University, Parkville VIC 3052, Australia

[3] Medicinal Chemistry, Institute of Pharmacy and Molecular Biotechnology, Heidelberg University, Im Neuenheimer Feld 364, 69120 Heidelberg, Germany

* Corresponding authors

phone: +61 2 61256507

e-mail: christoph.nitsche@anu.edu.au, gottfried.otting@anu.edu.au

Abstract

The Zika virus presents a serious risk for global health. Crystal structures of different constructs of the Zika virus NS2B-NS3 protease (NS2B-NS3pro) have been determined with the aim to provide a basis for rational drug discovery. In these structures, the C-terminal β-hairpin of NS2B, NS2Bc, was observed to be either disordered (open conformation) or bound to NS3pro complementing the substrate binding site (closed conformation). Enzymatically active constructs of flaviviral NS2B-NS3 proteases commonly used for inhibitor testing contain a covalent peptide linker between NS2B and NS3pro. Using a linked construct of Zika virus NS2B-NS3pro, we studied the location of NS2Bc relative to NS3pro in solution by pseudocontact shifts generated by a paramagnetic lanthanide tag attached to NS3pro. Both closed and open conformations were observed with different inhibitors. As the NS2B co-factor is involved in substrate binding of flaviviral NS2B-NS3 proteases, the destabilization of the closed conformation in the linked construct makes it an attractive tool to search for inhibitors that interfere with the formation of the enzymatically active, closed conformation.

Keywords

Inhibitor; NMR spectroscopy; NS2B-NS3 protease; pseudocontact shifts; Zika

Highlights

- A linked construct of the Zika virus NS2B-NS3 protease can assume open and closed conformations in solution
- Nuclear magnetic resonance (NMR) experiments with a paramagnetic tag confirm the closed conformation in solution
- A peptide linker between NS2B and NS3pro favours population of the open conformation
- The linked construct appears ideal to screen for inhibitors that prevent the enzymatically active fold of NS2B on NS3pro

Abbreviations

bZiPro, Zika virus NS2B-NS3 protease expressed in two individual parts; eZiPro, Zika virus NS2B-NS3 protease expressed with an enzymatic cleavage site between NS2B and NS3pro; gZiPro, Zika virus NS2B-NS3 protease expressed with a $Gly_4SerGly_4$ peptide linking NS2B with NS3pro; HSQC, heteronuclear single-quantum coherence; NMR, nuclear magnetic resonance; NS2B, part B of non-structural protein 2; NS3pro, protease domain of non-structural protein 3; PCS, pseudocontact shift; TROSY, transverse relaxation optimized spectroscopy

Introduction

The Zika virus recently emerged as a major threat to global health. It is a flavivirus that depends on the activity of a viral NS2B-NS3 protease, which thus is an attractive drug target. Owing to its high sequence and structure similarity with other flaviviral NS2B-NS3 proteases, such as the West Nile virus (WNV) (Chappell et al., 2008) and dengue virus (Nitsche et al., 2014) proteases, an inhibitor of the Zika virus protease could even display broad-spectrum activity against a wide range of flaviviruses (Boldescu et al., 2017). As full-length NS2B contains membrane-bound segments, an important advance was made when a soluble NS2B-NS3 construct was obtained for the dengue virus protease by covalently linking NS2B to the NS3 protease (NS3pro) via a covalent Gly_4-Ser-Gly_4 linker (Leung et al.; 2001). The same approach led to soluble NS2B-NS3pro constructs of the WNV and Zika virus proteases (Nall et al.; 2004, Lei et al., 2016). These constructs are enzymatically active and widely used for activity assays (Nitsche et al., 2014; 2017). There is no general agreement, however, whether the linked NS2B-NS3pro constructs are also the most suitable constructs for drug discovery.

NS2B is essential for full enzymatic activity, but crystal structures have found NS2B in very different conformations, open and closed, depending on the presence of inhibitors binding to the active site (Erbel et al., 2006; Noble et al., 2012; Lei et al., 2016; Chen et al., 2016a; Aleshin et al., 2007; Robin et al., 2009; Chandramouli et al., 2010; Hammamy et al., 2013). While the N-terminal segment of NS2B always forms an integral part of the β-barrel formed by NS3pro, the C-terminal part of NS2B, NS2Bc, forms a β-hairpin that tends to line the substrate binding site only in the presence of inhibitors (closed conformation), being dissociated from NS3pro in crystal structures without inhibitor (open conformation) (Erbel et al., 2006; Aleshin et

al. 2007; Chen et al., 2016a; Lee et al., 2017). In the case of the Zika virus protease, the β-hairpin of NS2Bc comprises residues 75*–87* (with the stars identifying residues of NS2B).

In solution, NMR data of the NS2B-NS3pro constructs from dengue virus, WNV and Zika virus showed NS2Bc in the closed conformation in the presence of inhibitors (Su et al., 2009; de la Cruz et al., 2011; Chen et al., 2014; Chen at al., 2016b; Zhang et al., 2016) and the closed conformation was also found in a WNV construct containing the Gly_4-Ser-Gly_4 linker without an inhibitor (Su et al., 2009). Solution NMR spectroscopy further indicated the closed conformation in constructs without covalent linkage between NS2B and NS3pro (Kim et al., 2013; de la Cruz et al., 2014). In the case of the Zika enzyme, however, solution NMR experiments revealed a more complex situation. A construct produced without covalent linkage between NS2B and NS3pro (named bZiPro) displayed the closed conformation in solution and the closed conformation was also captured in the single crystal (Zhang et al., 2016). For a related construct with an autocleavage site between NS2B and NS3pro (named eZiPro), however, the situation appears to be different in solution than in the single crystal: while the crystal structure showed the closed conformation, ^{15}N-relaxation data of NS2Bc indicated high mobility in solution, characteristic of the open conformation (Phoo et al. 2016). Although the substrate binding site in this construct was occupied by the C-terminal tetrapeptide of NS2B (residues 127-130), this was apparently not sufficient to maintain the closed conformation in solution.

Both eZiPro and bZiPro show two sets of cross-peaks for NS2B (Phoo et al., 2016; Zhang et al., 2016) which was attributed to the release of NS2B from the NS2B-NS3pro complex (Zhang et al., 2016). Greater stability of the protease would be expected for the classical construct containing the Gly_4-Ser-Gly_4 linker. This construct (referred to as gZiPro) has not been studied by NMR spectroscopy in the same detail as the unlinked constructs eZiPro and bZiPro. It

showed no change of the NMR spectrum with the classical protease inhibitor BPTI, suggesting that the covalent linkage prevents binding of the inhibitor (Phoo et al., 2016).

The question of open or closed conformation of the flaviviral NS2B-NS3 proteases is important for the inhibitor design. As crystalline environments can give different answers from the situation in solution, it is important to address the question by experiments under near-physiological conditions, i.e. in solution. To date, structural information on the Zika virus NS2B-NS3 protease in solution is limited to secondary structure. In this work, we investigated a chemically stable Zika virus construct containing the Gly_4-Ser-Gly_4 linker (gZiPro) by solution NMR spectroscopy with and without inhibitors, and determined the location of NS2Bc with respect to NS3pro by the use of pseudocontact shifts (PCS) induced by a paramagnetic lanthanide tag attached to NS3pro. The results show that gZiPro is a construct that can assume both the open and closed conformation in solution, making it an attractive tool for the discovery of antiviral drugs that can target either of these conformational states.

Experimental sections

Materials

Construct design

The gene of the gZiPro construct of the ZIKV NS2B-NS3 protease used in the present work was synthesized with codon optimization for expression in *E. coli* (Integrated DNA Technologies), based on the amino acid sequence of the South American isolate **Z1106033** (GenBank: **KU312312.1**; Enfissi et al., 2016). The construct included the 48 hydrophilic core residues of NS2B (residues 48*–95*, where a star identifies NS2B residues) followed by a $Gly_4SerGly_4$ linker, the 170 N-terminal residues of NS3 and a C-terminal His_6-tag. The three mutations

R95*A, K15N and R29G were introduced to eliminate potential auto-cleavage sites and increase protein stability. To allow site-specific ligation of a lanthanide tag to a single, engineered cysteine residue, the two native cysteine residues 80 and 143 were mutated to serine. Apart from the K15N and the cysteine-to-serine mutations, our construct is closely related to that used for the crystal structure **5LC0** (Lei et al., 2016). The gene was cloned between the *Nde*I and *Eco*RI sites of the T7 vector pETMCSI (Neylon et al., 2000). In addition, the mutant T27C was prepared for attaching a lanthanide tag to residue 27. Figure S1 compares the amino acid sequences of our construct and previously used gZiPro constructs.

Protein sample preparation

Uniformly isotope-labelled protein was produced in *E. coli* BL21(DE3) using a high-cell density protocol (Sivashanmugam et al., 2009). Following induction with 1 mM IPTG at an OD_{600} value of about 0.5–0.8, the cells were incubated overnight at 25 °C. Cells were grown in M9 medium (6 g/l Na_2HPO_4, 3 g/l KH_2PO_4, 0.5 g/l NaCl) supplied with 1 g/l $^{15}NH_4Cl$) for uniform ^{15}N-labelling and in $^{13}C/^{15}N$-labelled Spectra 9 medium (Cambridge Isotope Laboratories, Tewksbury, USA) for double-labelling. The cells were pelleted by centrifuging at 5,000 *g* for 10 minutes and lysed by passing twice through a French Press (SLM Aminco, USA) at 830 bars. The cell lysate was centrifuged for 1 h at 34,000 *g* and supernatant was loaded on to a 5 ml Co-NTA column (GE Healthcare, USA) pre-equilibrated with buffer A (50 mM Tris-HCl, pH 7.5, 150 mM NaCl, 5% glycerol). The protein was eluted with buffer B (50 mM Tris-HCl, pH 7.5, 150 mM NaCl, 300 mM imidazole, 5% glycerol) and fractions were analyzed by 12% SDS-PAGE. Finally, the buffer was exchanged for NMR buffer (20 mM MES, pH 6.5, 150 mM NaCl) and 10% D_2O was added for NMR measurements.

Selectively isotope-labelled protein samples and samples with site-directed mutations for resonance assignments were prepared by cell-free protein synthesis (Ozawa et al., 2004; Apponyi et al., 2008) and purified using a 1 ml His GraviTrap^{TM} TALON column (GE Healthcare, USA). Cell-free synthesis enabled efficient production of selectively isotope-labelled samples (Table S1), including samples where each of the twenty amino acids except Glu, Gln, Cys and Pro was selectively labelled with ^{15}N. Cell-free synthesis from PCR-amplified DNA (Wu et al., 2007) was also used to obtain site-specific resonance assignments of all eight isoleucine residues by individual mutation to valine in eight ^{15}N-isoleucine-labelled samples. Similarly, the assignments of valine residues was probed by mutating 20 of 24 valine residues to isoleucine in 20 ^{15}N-valine-labelled samples.

The ^{15}N-labelled T27C mutant of Zika NS2B-NS3pro was tagged with lanthanide ions by incubation at 25 °C overnight in the presence of three-fold excess C2 tag (Graham et al. 2011; de la Cruz et al. 2011) loaded with either paramagnetic Tm^{3+}, Tb^{3+} or diamagnetic Y^{3+}. Following the tagging reaction, the samples were washed with NMR buffer using a centrifugal filter unit (Amicon Ultra, molecular weight cut-off 10 kDa; Millipore, Billerica, USA) to remove unbound tag.

Inhibitors

Figure 1 shows the inhibitors used. Inhibitors **1** (corresponding to cn-716) and **2** (corresponding to cn-729) were synthesized as described previously (Nitsche et al., 2017). Inhibitor **3** (Lim et al., 2016) was purchased from Sigma-Aldrich. Protein samples with inhibitors were prepared by adding a 1.5-fold of excess of inhibitor **1** and **2** and a four-fold of excess of inhibitor **3**.

NMR spectroscopy

NMR spectra were recorded at 25 °C, using 600 MHz and 800 MHz Bruker Avance NMR spectrometers equipped with cryoprobes. 3D HNCA and 3D NOESY-^{15}N-HSQC experiments were performed with protein concentrations of 0.5–0.8 mM in 5 mm NMR tubes. 2D NMR spectra were recorded with 0.1–0.2 mM samples in 3 mm NMR tubes.

Backbone resonance assignments

For backbone resonance assignments, the 3D HNCA and NOESY-^{15}N-HSQC spectra were supplemented by [^{15}N,^{1}H]-HSQC spectra of selectively isotope-labelled samples and samples with site-directed mutations. The assignments of NS2Bc residues were supported by recording 2D BEST-TROSY-HNCO spectra (Solyom et al., 2013).

Δχ-tensor fits

Pseudocontact shifts (PCS), $\Delta\delta^{PCS}$, were measured as the difference in amide proton chemical shifts observed in NMR spectra recorded with and without paramagnetic metal ion (in ppm). The PCSs were used to fit magnetic susceptibility anisotropy ($\Delta\chi$) tensors to the crystal structure coordinates using the equation

$$\Delta\delta^{PCS} = 1/(12\pi r^3)[\Delta\chi_{ax}(3\cos^2\theta - 1) + 1.5\Delta\chi_{rh}\sin^2\theta\cos 2\phi] \quad (1)$$

where r is the distance of the nuclear spin from the metal ion, $\Delta\chi_{ax}$ and $\Delta\chi_{rh}$ are the axial and rhombic components of the $\Delta\chi$ tensor, and θ and ϕ are the polar angles describing the position of the nuclear spin with respect to the principal axes of the $\Delta\chi$ tensor. The fits were performed

using the program Numbat (Schmitz et al., 2008). The quality of the fits were determined by the quality factor *Q*, which was calculated as the root mean square deviation between experimental and back-calculated PCSs divided by the root mean square of the the experimental PCSs.

Chemical shift changes

Chemical shift changes, Δδ, were calculated using the equation

$$\Delta\delta = \mathrm{Sqrt}[(\Delta\delta_H)^2 + 0.2(\Delta\delta_N)^2] \quad (2)$$

where $\Delta\delta_H$ and $\Delta\delta_N$ are, respectively, the changes measured in the ^{1}H and ^{15}N dimensions of [^{15}N,^{1}H]-HSQC spectra.

Results

NMR resonance assignments

The protein was produced in good yields of about 74 mg per litre medium *in vivo* and about 2 mg per mL reaction mixture in cell-free synthesis, but the NMR resonance assignments of the free protein were made difficult by a tendency for precipitation, spectral overlap and variable peak intensities for different amino acid residues. To assign the backbone amide resonances, we supplemented 3D NMR data with 2D [^{15}N,^{1}H]-correlation spectra of selectively isotope-labelled protein prepared by cell-free synthesis. [^{15}N,^{1}H]-HSQC spectra were recorded of 16 different samples, in which only a single residue type was labelled with ^{15}N. In addition, site-specific resonance assignments of isoleucine residues were obtained by isoleucine-to-valine mutations in ^{15}N-isoleucine-labelled samples. Similarly, 20 out of 24 valine residues were individually mutated to isoleucine to assign their amide cross-peaks. Finally, 2D HN(CO) spectra were

recorded of eight samples selectively labelled with ^{15}N and ^{13}C (Table S1) to identify the [^{15}N,^{1}H]-HSQC cross-peaks of individual residues following a ^{13}C-labelled residue (Kainosho and Tsuji, 1982). The final assignment comprised the resonances of 174 out of 216 non-proline backbone amides (Figure S2). The cross-peak assignments were confirmed and supported by comparison with the assignments published for the slightly different construct eZiPro (Phoo et al., 2016).

In the course of titration with inhibitor **1**, NMR signals of NS2Bc disappeared while new resonances appeared, indicating that the exchange between inhibitor-bound and free protein is slow on the NMR time scale. This was expected, as inhibitor **1** binds with low nanomolar affinity, assisted by reversible covalent bond formation of its boronate group with the active-site serine (residue 135; Lei et al., 2016). In contrast to previous results obtained with eZiPro and bZiPro (Phoo et al., 2016; Zhang et al., 2016), NS2B did not display a set of cross-peaks corresponding to free NS2B in the presence of inhibitor **1**. Figure 2 shows that, while many cross-peaks changed only little following addition of inhibitor **1**, others displayed large changes in chemical shifts, making it necessary to obtain new resonance assignments. 2D HN(CO) spectra of the selectively ^{15}N- and ^{13}C-labelled samples used for resonance assignments of the free protein (Table S1) were used to assign the new cross-peaks of NS2Bc appearing after addition of inhibitor **1**. The chemical shifts of these peaks proved to be close to the better dispersed set of cross-peaks reported previously for eZiPro (Phoo et al., 2016).

NS2Bc-NS3pro association in the presence of inhibitor 1

To assess the location of NS2Bc with respect to NS3pro, we attached the C2 lanthanide tag at position 27 in the T27C mutant. Loaded with either Tm^{3+} or Tb^{3+}, this tag tends to shift the

cross-peaks in opposite directions relative to the diamagnetic reference obtained with C2-Y^{3+}, facilitating the assignment of the paramagnetic NMR spectra (Nitsche and Otting, 2017). PCSs with the C2-Tm^{3+} tag were observed for over thirty cross-peaks (Table S2, Figure 3), which allowed determination of the magnetic susceptibility anisotropy ($\Delta\chi$) tensor using equation 1 (Table S3). The tensor predicts PCSs of about -0.1 ppm at the site of NS2Bc, if NS2Bc were in the closed conformation as in the crystal structures (Figure 4). The experimentally observed PCSs of residues 55*–86* in NS2B indeed correlated closely with the predicted PCSs (Figure 5), indicating that, in the presence of inhibitor **1**, the closed conformation observed in the crystal structure **5LC0** is also the prevalent conformation in solution. The closed conformation was also supported by similar $R_2(^{15}N)$ relaxation rates observed for residues in NS2Bc and NS3pro (data not shown). Judging by the quality factor of the $\Delta\chi$-tensor fits, the closed conformation of the structure **5LC0** explains the PCSs measured with inhibitor **1** better than the open conformation of the structure **5T1V** (Table S3).

NS2Bc-NS3pro association in the absence of inhibitors

To probe the conformation of gZiPro in the inhibitor-free state, we again used the PCSs generated by C2-Ln^{3+} tags attached to position 27 in the T27C mutant (Figure S3). Good $\Delta\chi$-tensor fits were obtained (Figure S4 and Table S3), but while the amide cross-peaks of residues 71*, 81*, 82* and 85* of NS2B could be observed in the presence of the diamagnetic C2-Y^{3+} tag, they disappeared in the presence of a paramagnetic C2 tag. The effect can be explained by excessive line broadening due to dislocation of NS2Bc from its usual site on NS3pro. This dislocation could bring NS2Bc into proximity of the paramagnetic tags where it would be exposed to paramagnetic relaxation enhancements. In addition, the signals could be broadened

by chemical exchange between environments with different PCSs, if the exchange occurs in the intermediate time regime. For the observable PCSs, the open conformation of the crystal structure **5T1V** fitted the PCSs as well as the closed conformation of the crystal structure **5LC0**.

Dissociation of NS2Bc from NS3pro was supported by $R_2(^{15}N)$ relaxation rates, which were on average 14 s^{-1} and about four times smaller than for NS3pro (data not shown). Much slower relaxation rates in NS2Bc versus NS3pro have similarly been reported for the eZiPro construct (Phoo et al., 2016). In addition, the chemical shifts of all assigned amide protons of NS2Bc were in the range 7.6 – 8.6 ppm, which is characteristic of chemical shifts in flexibly disordered proteins. The chemical shifts were also close to those reported by Zhang et al. (2016) for free NS2B peptide. Therefore, the gZiPro construct used in this work assumes an open conformation in solution, if no high-affinity inhibitor is present.

Complexes with inhibitors 2 and 3

Titration with the inhibitor **2**, which differs from inhibitor **1** by an additional *t*-butyl group and an alternative basic P_2 side chain (Figure 1), led to the disappearance of the cross-peaks of NS2Bc and of many of the NS3pro resonances, suggesting excessive broadening by chemical exchange in the intermediate time regime (Figure S5). This result indicates that the structure of the complex is destabilized by the steric clash between the *t*-butyl group and the loop comprising residues 154–161 in NS3pro, which is predicted by the crystal structure **5LC0**. Previously reported IC_{50} values of inhibitor **2** versus inhibitor **1** indicated weaker binding of inhibitor **2** (2.1 versus 0.25 nM; Nitsche et al., 2017). While the ^{1}H-NMR signal of the *t*-butyl group of inhibitor **2** could readily be observed in the complex with the dengue virus protease (Chen et al. 2016b), it was too broad to be resolved in the complex with the Zika virus protease.

Titration with the inhibitor **3** also produced chemical shift changes and line-broadening effects (Figure S6). The inhibitor binds in slow exchange. Signals of His51 and Tyr130 in the substrate binding site disappeared, and chemical shift changes were observed not only near the substrate binding site but also on the far side of the protease (Figure 6A). A wide distribution of chemical shift changes was also observed with inhibitor **1**, which is known to bind at the active site (Figure 6B). Therefore, the data suggest that inhibitor **3**, which is active against a range of different serine proteases, binds at the active site and the chemical shift changes observed elsewhere in the protease reflect allosteric conformational changes. There is no evidence, however, that inhibitor **3** induces the closed conformation, as the chemical shifts of residues in NS2Bc remained unaffected (Figure S7).

Discussion

Six different crystal structures of the Zika virus protease have been published and all but two of them show the closed conformation, irrespective of the presence or absence of ligands in the substrate binding site (Lei et al., 2016; Phoo et al., 2016; Zhang et al., 2016), with no electron density observed for NS2Bc in the open conformation (Chen et al., 2016a; Lee et al., 2017). A different situation prevails in the case of the related dengue and West Nile virus proteases, for which crystal structures in the absence of inhibitors invariably show open conformations, where NS2Bc is dissociated from NS3pro (Erbel et al., 2006; Aleshin et al., 2007; Chandramouli et al., 2010). In the case of the Zika virus protease, the state of NS2Bc in solution has been addressed by relaxation experiments performed by NMR spectroscopy, indicating that NS2Bc is associated with NS3pro in the construct bZiPro, which has no covalent linkage between NS2B and NS3 (Zhang et al., 2016). Similarly, in the absence of a linker peptide connecting NS2B and NS3, the

closed state has earlier been reported for the dengue virus protease (Kim et al., 2013; de la Cruz et al., 2014). Unexpectedly, however, much slower relaxation rates for NS2Bc than NS3pro were reported for the autoproteolytically cleaved construct eZiPro, indicating dissociation of NS2Bc from NS3pro (Phoo et al., 2016). The authors did not report which of the two sets of cross-peaks observed for NS2B were used for relaxation measurements.

The present work used pseudocontact shifts in order to assess the actual location of NS2Bc in a linked gZiPro construct of the Zika virus protease in solution. While PCSs were predicted for NS2Bc in the closed conformation and, in fact, observed in the presence of inhibitor **1**, NS2Bc resonances disappeared in the presence of paramagnetic tags, indicating chemical exchange broadening. This can be explained, if NS2Bc exchanges between locations of different PCSs in various open conformations. Increased motions are also supported by the relaxation and chemical shift data. Notably, however, not all inhibitors induce the closed conformation, as shown by the results obtained with inhibitor **3**.

The open conformation is most likely promoted by the artificial linker between NS2B and NS3pro. In the wild-type enzyme, no such linkage exists due to an autoproteolytic cleavage site. Formally, the linker in gZiPro is represented by only nine residues ($Gly_4SerGly_4$), which should not be able to span the distance between the last residue of NS2B and the first residue of NS3 observed in the crystal structures (about 45 Å, see Figure 4). Notably, however, none of the crystal structures report electron density for the N-terminal 14 residues of NS3 and flexible disorder of the 17 N-terminal residues was also indicated by greatly reduced $R_2(^{15}N)$ and increased $R_1(^{15}N)$ relaxation rates in the unlinked construct eZiPro (Phoo et al., 2016). These residues must thus be included in the flexible link between NS2B and NS3. In fully extended conformation, 31 residues could span over 100 Å.

As NS2Bc binds only weakly to NS3pro, the open conformation appears as a possible target for an inhibitor that, by preventing formation of the closed conformation, greatly diminishes the activity of the protease. By biasing the equilibrium between open and closed conformation towards the open state, the gZiPro construct could be uniquely suited to probe whether an inhibitor induces the closed conformation or binds to the open conformation. For quantitative measurements of dissociation constants, gZiPro also has the distinctive advantage of not releasing NS2B into the solution, in contrast to the constructs eZiPro and bZiPro. The relevance of gZiPro as a research tool has very recently been demonstrated by the identification of bromocriptine as an inhibitor of the Zika virus protease with similar activity both in biochemical and cellular assays (Chan et al., 2017).

Acknowledgements

We thank Professor Rolf Hilgenfeld for valuable comments regarding the construct design. C.N. thanks the Alexander von Humbolt Foundation for a Feodor-Lynen fellowship. Financial support by the Australian Research Council is gratefully acknowledged. C.K. acknowledges support by the Deutsche Forschungsgemeinschaft, grant KL 1356/3.

References

Aleshin, A.E., Shiryaev, S.A., Strongin, A.Y., Liddington, R.C., 2007. Structural evidence for regulation and specificity of flaviviral proteases and evolution of the *Flaviviridae* fold. Protein Sci. 16, 795–806.

Apponyi, M.A., Ozawa, K., Dixon, N. E., Otting, G., 2008. Cell-free protein synthesis for analysis by NMR spectroscopy. Methods Mol. Biol. 426, 257–268.

Boldescu, V., Behnam, M.A.M., Vasilakis, N., Klein, C.D., 2017. Broad-spectrum agents for flaviviral infections: Dengue, Zika and beyond. Nat. Rev. Drug Discov., in press.

Chan, J.F.-W., Chik, K.K.-H., Yuan, S., Yip, C.C.-Y., Zhu, Z., Tee, K.-M., Tsang, J.O-L., Chan, C.C.-S., Poon, V.K.-M., Lu, G., Zhang, A.J., Lai, K.-K., Chan, K.-H., Kao, R.Y.-T., Yuen, K.-Y., 2017. Novel antiviral activity and mechnism of bromocriptine as a Zika virus NS2B-NS3 protease inhibitor. Antiviral Res., doi:10.1016/j.antiviral.2017.02.002.

Chandramouli, S., Joseph, J.S., Daudenarde, S., Gatchalian, J., Cornillez-Ty, C., Kuhn, P., 2010. Serotyp-specific structural differences in the protease-cofactor complexes of the dengue virus family. J. Virol. 84, 3059–3067.

Chappell, K.J., Stoermer, M.J., Fairlie, D.P., Young, P.R., 2008. West Nile virus NS2B/NS3 protease as an antiviral target. Curr. Med. Chem. 15, 2771–2784.

Chen, X., Yang, K., Wu, C., Chen, C., Hu, C., Buzovetsky, O., Wang, Z., Ji, X., Xiong, Y., Yang, H., 2016a. Mechanisms of activation and inhibition of Zika virus NS2B-NS3 protease. Cell Res. 26, 1260–1263.

Chen, W.-N., Loscha, K.V., Nitsche, C., Graham, B., Otting, G., 2014. The dengue virus NS2B-NS3 protease retains the closed conformation in the complex with BPTI FEBS Lett. 588, 2206–2211.

Chen, W.-N., Nitsche, C., Pilla, K.B., Graham, B., Huber, T., Klein, C.D., Otting, G., 2016b. Sensitive NMR approach for determining the binding mode of tightly binding ligand molecules to protein targets. J. Am. Chem. Soc. 138, 4539–4546.

de la Cruz, L., Nguyen, T.H., Ozawa, K., Shin, J., Graham, B., Huber, T., Otting, G., 2011. Binding of low molecular weight inhibitors promotes large conformational changes in the dengue virus NS2B-NS3 protease: fold analysis by pseudocontact shifts. J. Am. Chem. Soc. 133, 19205–19215.

de la Cruz, L., Chen, W.N., Graham, B., Otting, G., 2014. Binding mode of the activity-modulating C-terminal segment of NS2B to NS3 in the dengue virus NS2B-NS3 protease. FEBS J. 281, 1517–1533.

Enfissi, A., Codrington, J., Roosblad, J., Kazanji, M., Roussetet, D., 2016. Zika virus genome from the Americas. Lancet 387, 227–228.

Erbel, P., Schiering, N., D'Arcy, A., Renatus, M., Kroemer, M., Lim, S.P., Yin, Z., Keller, T.H., Vasudevan, S.G., Hommel, U., 2006. Structural basis for the activation of flaviviral NS3 proteases from dengue and West Nile virus. Nat. Struct. Mol. Biol. 13, 372–373.

Graham, B., Loh, C.T., Swarbrick, J.D., Ung, P., Shin, J., Yagi, H., Jia, X., Chhabra, S., Pintacuda, G., Huber, T., Otting, G., 2011. A DOTA-amide lanthanide tag for reliable generation of pseudocontact shifts in protein NMR spectra. Bioconjugate Chem. 22, 2118–2125.

Hammamy, M.Z., Haase, C., Hammami M., Hilgenfeld, R., Steinmetzer, T., 2013. Development and characterization of new peptidomimetic inhibitors of the West Nile virus NS2B-NS3 protease. ChemMedChem 8, 231–241.

Kainosho, M., Tsuji, T., 1982. Assignment of the three methionyl carbonyl carbon resonances in *Streptomyces* subtilisin inhibitor by a carbon-13 and nitrogen-15 double-labeling technique. A new strategy for structural studies of proteins in solution. Biochemistry 21, 6273–6279.

Kim, Y.M., Gayen, S., Kang, C., Joy, J., Huang, Q., Chen, A.S., Wee, J.L., Ang, M.J., Lim, H.A., Hung, A.W., Li, R., Noble, C.G., Lee le, T., Yip, A., Wang, Q.Y., Chia, C.S., Hill, J., Shi, P.Y., Keller, T.H., 2013. NMR analysis of a novel enzymatically active unlinked dengue NS2B-NS3 protease complex. J. Biol. Chem. 288, 12891–12900.

Lee, H., Ren, J., Nocadello, S., Rice, A.J., Ojeda, I., Light, S., Minasov, G., Vargas, J., Nagarathnam, D., Anderson, W.F., Johnson, M.E., 2017. Identification of novel small molecule inhibitors against NS2B/NS3 serine protease from Zika virus. Antiviral Res. 139, 49–58.

Lei, J., Hansen, G., Nitsche, C., Klein, C. D., Zhang, L. L., Hilgenfeld, R., 2016. Crystal structure of Zika virus NS2B-NS3 protease in complex with a boronate inhibitor. Science 353, 503–505.

Leung, D., Schroder, K., White, H., Fang, N.X., Stoermer, M.J., Abbenante, G., Martin, J.L., Young, P.R., Fairlie, D.P., 2001. Activity of recombinant dengue 2 virus NS3 protease in the presence of a truncated NS2B co-factor, small peptide substrates, and inhibitors. J. Biol. Chem. 276, 45762–45771.

Lim, L., Roy, A., Song, J., 2016. Identification of a Zika NS2B-NS3pro pocket susceptible to allosteric inhibition by small molecules including qucertin rich in edible plants. bioRxiv, doi: 10.1101/078543.

Nall, T.A., Chappell, K.J., Stoermer, M.J., Fang, N.X., Tyndall, J.D., Young, P.R., Fairlie, D.P., 2004. Enzymatic characterization and homology model of a catalytically active recombinant West Nile virus NS3 protease. J. Biol. Chem. 279, 48535–48542.

Neylon, C., Brown, S.E., Kralicek, A.V., Miles, C.S., Love, C.A., Dixon, N.E., 2000. Interaction of the *Escherichia coli* replication terminator protein (Tus) with DNA: a model derived from DNA-binding studies of mutant proteins by surface plasmon resonance. Biochemistry 39, 11989–11999.

Nitsche, C., Holloway, S., Schirmeister, T., Klein, C.D., 2014. Biochemistry and medicinal chemistry of the dengue virus protease. Chem. Rev. 114, 11348–11381.

Nitsche, C. and Otting, G., 2017. Pseudocontact shifts in biomolecular NMR using paramagnetic metal tags. Prog. NMR Spectr. 98-99, 20-49.

Nitsche, C., Zhang, L., Weigel, L.F., Shilz, J., Graf, D., Bartenschlager, R., Hilgenfeld, R., Klein, C.D., 2017. Peptide–boronic acid inhibitors of flaviviral proteases: medicinal chemistry and structural biology. J. Med. Chem. 60, 511–516.

Noble, C.G., Seh, C.C., Chao, A.T., Shi, P.Y., 2012. Ligand-bound structures of the dengue virus protease reveal the active conformation. J. Virol. 86, 438–446.

Ozawa, K., Headlam, M. J., Schaeffer, P. M., Henderson, B. R., Dixon, N. E., Otting, G., 2004. Optimization of an *Escherichia coli* system for cell-free synthesis of selectively ^{15}N-labelled proteins for rapid analysis by NMR spectroscopy. Eur. J. Biochem. 271, 4084–4093.

Phoo, W.W., Li, Y., Zhang, Z., Lee, M.Y., Loh, Y.R., Tan, Y.B., Ng, E.Y., Lescar, J., Kang, C., Luo, D., 2016. Structure of the NS2B-NS3 protease from Zika virus after self-cleavage. Nat. Commun. 7, 13410.

Robin, G., Chappell, K., Stoermer, M.J., Hu, S.-H., Young, P. R., Fairlie, D.P., Martin, J.L., 2009. Structure of West Nile virus NS3 protease: ligand stabilization of the catalytic conformation. J. Mol. Biol. 385, 1568–1577.

Schmitz, C., Stanton-Cook, M.J., Su, X.-C., Otting, G., Huber, T., 2008. Numbat: an interactive software tool for fitting $\Delta\chi$-tensors to molecular coordinates using pseudocontact shifts. J. Biomol. NMR 41, 179–189.

Sivashanmugam, A., Murray, V., Cui, C. X., Zhang, Y. H., Wang, J. J., Li, Q. Q., 2009. Practical protocols for production of very high yields of recombinant proteins using *Escherichia coli*. Protein Sci. 18, 936–948.

Solyom, Z., Schwarten, M., Geist, L., Konrat, R., Willbold, D., Brutscher, B., 2013. BEST-TROSY experiments for time-efficient sequential resonance assignment of large disordered proteins, J. Biomol. NMR 55, 311–321.

Su, X.C., Ozawa, K., Qi, R., Vasudevan, S.G., Lim, S.P., Otting, G., 2009. NMR analysis of the dynamic exchange of the NS2B cofactor between open and closed conformations of the West Nile virus NS2B-NS3 protease. PLoS Negl. Trop. Dis. 3, e561.

Wu, P.S.C., Ozawa, K., Lim, S. P., Vasudevan, S., Dixon, N. E., Otting, G., 2007. Cell-free transcription/translation from PCR amplified DNA for high-throughput NMR studies. Angew. Chemie Int. Ed. 46, 3356–3358.

Zhang, Z., Li, Y., Loh, Y.R., Phoo, W.W., Hung, A.W., Kang, C., Luo, D., 2016. Crystal structure of unlinked NS2B-NS3 protease from Zika virus. Science 354, 1597–1600.

Figure Captions

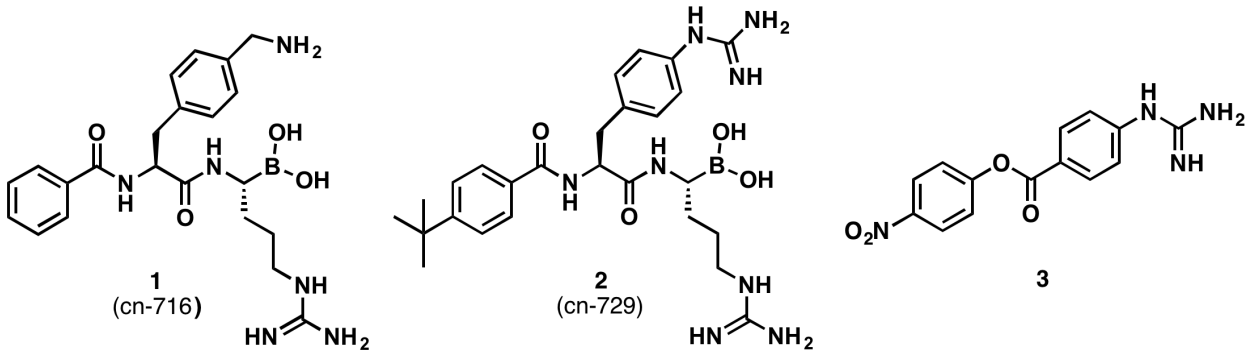

Figure 1. Inhibitors used in the present work. Inhibitors **1** and **2** have been published previously under the names cn-716 and cn-729 (Lei et al., 2016; Nitsche et al., 2017) and inhibitor **3** has been reported by Lim et al. (2016).

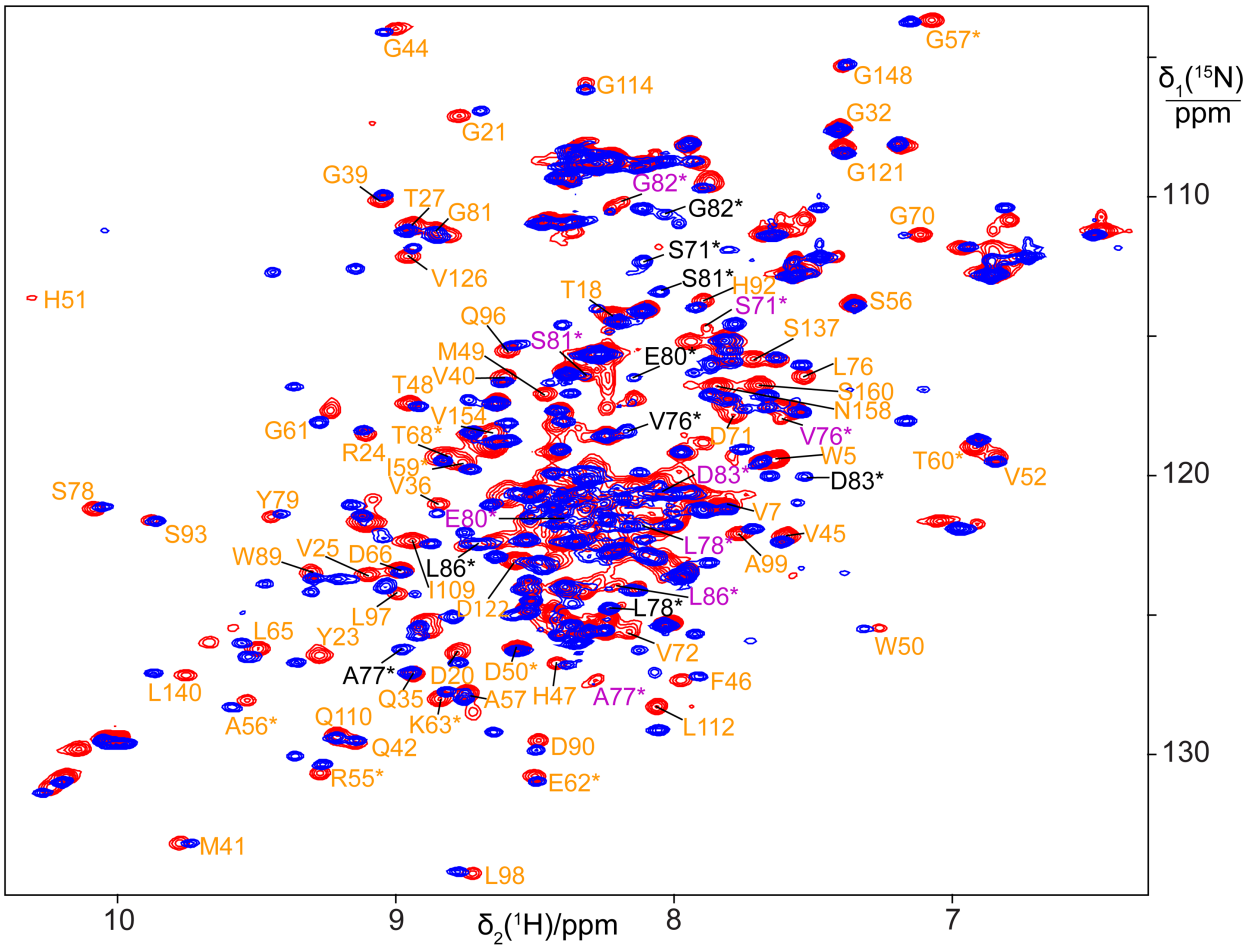

Figure 2. Superimposition of [^{15}N,^{1}H]-HSQC spectra of 0.12 mM solutions of uniformly ^{15}N-labelled Zika virus NS2B-NS3 protease in NMR buffer (20 mM MES, pH 6.5) with (blue spectrum) and without inhibitor **1** (red spectrum). The inhibitor was added in 1.5-fold excess. Assignments are shown for resolved cross-peaks that were changed by the presence of inhibitor. Cross-peaks of NS2B are marked with a star. Magenta and black labels highlight cross-peaks of NS2Bc residues without and with the inhibitor, respectively. N-H cross-peaks of side-chains were assigned only by residue type. The group of five cross-peaks near (δ_1 = 130 ppm; δ_2 = 10.1 ppm) are from tryptophan indol rings of which Trp50 is nearest to the substrate binding site.

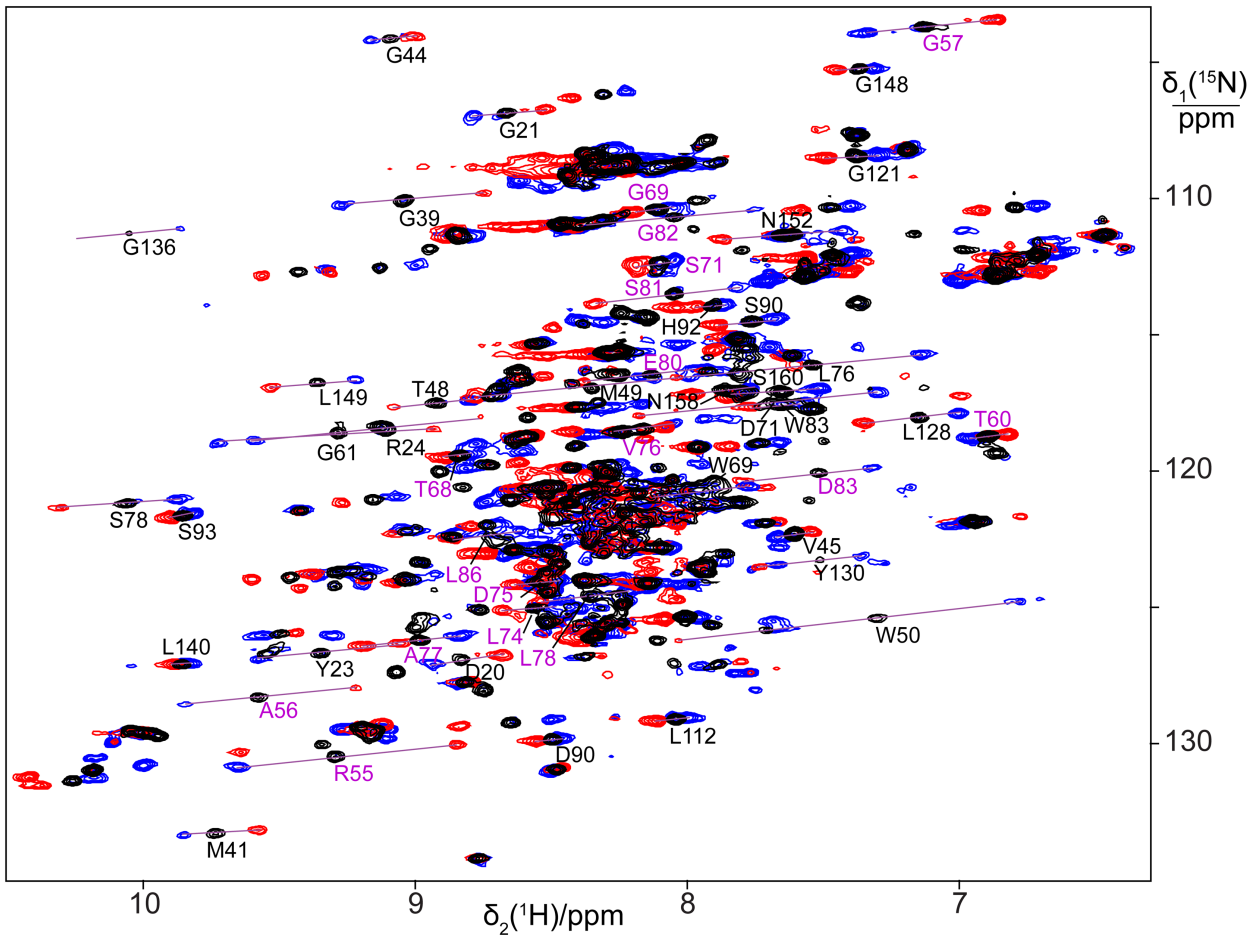

Figure 3. Superimposition of [^{15}N,^{1}H]-HSQC spectra of 0.12 mM solutions of the T27C mutant of Zika virus NS2B-NS3pro tagged with C2-Tm^{3+} (blue), C2- Tb^{3+} (red) or diamagnetic C2-Y^{3+}

(black) in the presence of a 1.5-fold excess of inhibitor **1**. Cross-peak assignments of NS3pro and NS2B are labelled in black and magenta, respectively.

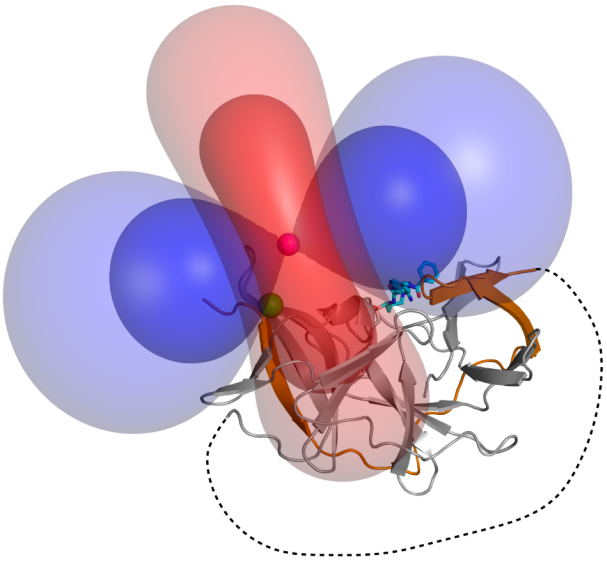

Figure 4. PCS isosurfaces representing the $\Delta\chi$ tensor obtained with the C2-Tm^{3+} tag attached at position 27. The isosurfaces correspond to PCSs of 1 ppm (dark blue), 0.1 ppm (light blue), -1 ppm (dark red) and -0.1 ppm (light red), and are plotted on the crystal structure of the Zika virus NS2B-NS3 protease in complex with inhibitor **1** (PDB ID: **5LC0**). The metal position is shown as a magenta sphere and the C^{α} atom of the tag attachment site is indicated by a green sphere. The inhibitor **1** is represented by a stick representation. 31 residues, indicated by a dotted line and including the $Gly_4SerGly_4$ linker, connect the C-terminus of NS2B with the N-terminus of NS3pro, but no coordinates are reported for these disordered residues in the crystal structure.

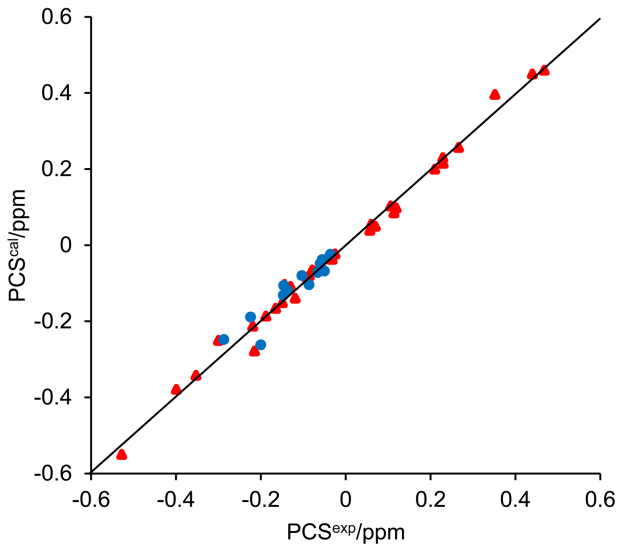

Figure 5. Correlation between back-calculated and experimental PCSs of backbone amide protons of gZiPro with inhibitor **1**. The PCSs of residues used to fit the $\Delta\chi$ tensor are indicated by red triangles. They include all PCSs measured for NS3pro and residues 55*, 56*, 57* and 60* of NS2B. PCSs of NS2B residues between residues 68* and 86* (including NS2Bc) are indicated by blue circles. These PCSs are well explained by the $\Delta\chi$ tensor, although they were not used in the $\Delta\chi$-tensor fit.

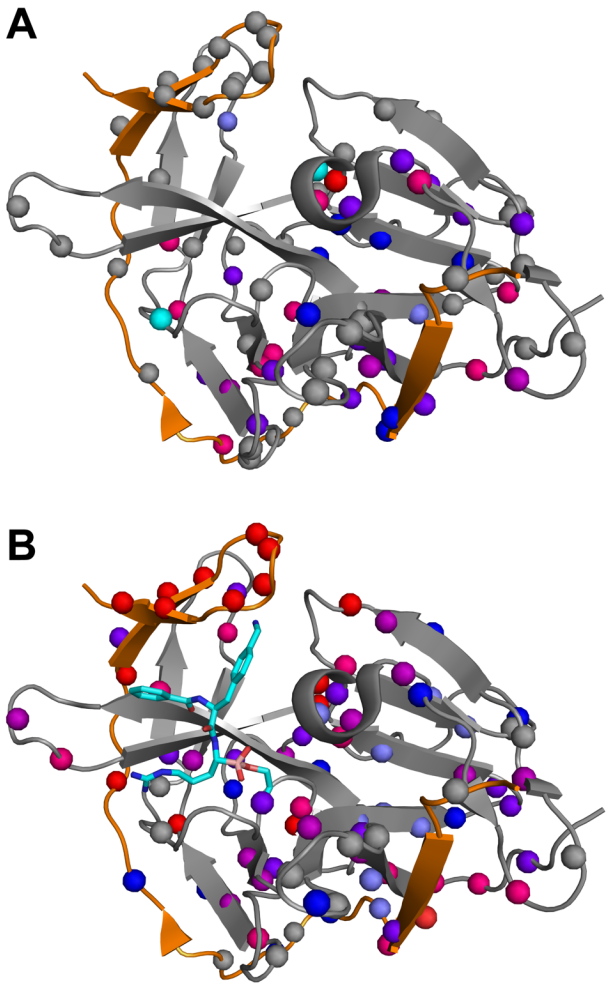

Figure 6. Crystal structure **5LC0** of the Zika virus NS2B-NS3 protease with spheres highlighting the backbone amides for which chemical shift changes upon binding of inhibitor could be assessed. The magnitude of chemical shift change is depicted on a colour scale from red (>0.1 ppm) to blue (>0.01 ppm). Grey spheres indicate amides without significant change in chemical shift (<0.01 ppm). (A) Results for inhibitor **3**. The amide protons of His51 and Tyr130, for which the [^{15}N,^{1}H]-cross-peaks disappear rather than shift upon titration with the inhibitor, are highlighted by cyan spheres. (B) Results for inhibitor **1**.